Direct Probing by Atomic Force Microscopy of the Cell Surface Softness of a Fibrillated and Nonfibrillated Oral Streptococcal Strain

Henny C. van der Mei,* Henk J. Busscher,* Rolf Bos,* Joop de Vries,* Christophe J. P. Boonaert,† and Yves F. Dufrêne†

*Department of Biomedical Engineering, University of Groningen, Antonius Deusinglaan 1, 9713 AV Groningen, the Netherlands, and †Unité de Chimie des Interfaces, Université Catholique de Louvain, B-1348 Louvain-la-Neuve, Belgium

ABSTRACT In this paper, direct measurement by atomic force microscopy (AFM) of the cell surface softness of a fibrillated oral streptococcal strain *Streptococcus salivarius* HB and of a nonfibrillated strain *S. salivarius* HBC12 is presented, and the data interpretation is validated by comparison with results from independent techniques. Upon approach of the fibrillated strain in water, the AFM tip experienced a long-range repulsion force, starting at ~100 nm, attributed to the compression of the soft layer of fibrils present at the cell surface. In 0.1 M KCl, repulsion was only experienced when the tip was closer than ~10 nm, reflecting a stiffer cell surface due to collapse of the fibrillar mass. Force-distance curves indicated that the nonfibrillated strain, probed both in water and in 0.1 M KCl, was much stiffer than the fibrillated strain in water, and a repulsion force was experienced by the tip at close approach only (20 nm in water and 10 nm in 0.1 M KCl). Differences in cell surface softness were further supported by differences in cell surface morphology, the fibrillated strain imaged in water being the only specimen that showed characteristic topographical features attributable to fibrils. These results are in excellent agreement with previous indirect measurements of cell surface softness by dynamic light scattering and particulate microelectrophoresis and demonstrate the potential of AFM to directly probe the softness of microbial cell surfaces.

INTRODUCTION

Microbial cell surfaces differ substantially from the surfaces of inert solids. Often, microbial cell surfaces show chemical heterogeneity, in combination with arrays of structural surface appendages. The protruding nature of these appendages and their specific chemistry enable microorganisms to adhere to different types of substrata, despite the fact that overall electrostatic interactions are generally not favorable for microbial adhesion to occur (Busscher et al., 2000). Electron microscopy on negatively stained bacteria has indicated appendages on streptococcal cell surfaces called fibrils, which can be as long as several micrometers, but on the other hand, nonfibrillated streptococcal strains showing bald surfaces exist as well (Handley, 1990).

Because of their fibrillated cell surface, streptococci are typical examples of "soft particles." The softness of streptococcal cell surfaces depends on environmental parameters, such as pH and ionic strength. Dynamic light scattering has demonstrated that the diffusion coefficient of a fibrillated oral streptococcal strain, *Streptococcus salivarius* HB, was higher in low pH suspensions than in high pH suspensions because of collapse of the fibrils, whereas the diffusion coefficient of a bald, nonfibrillated strain, *S. salivarius* HBC12, varied less with pH (Van der Mei et al., 1994). Recently (Bos et al., 1998), we compared the softness of both strains by measuring their electrophoretic mobility as a function of ionic strength and interpreting the electrophoretic mobility measured as originating from a combination of surface layer charges and membrane fixed charges. According to the theory described by Ohshima for the electrophoretic mobility of soft, polyelectrolyte-covered particles (Ohshima, 1994, 1995; Ohshima and Kondo, 1991), soft particles can be characterized by the softness of the surface layer $1/\lambda$ and the density of charged groups in the polyelectrolyte layer zN. The fibrillated strain *S. salivarius* HB appeared twice as soft in this analysis ($1/\lambda = 1.4$ nm) than the nonfibrillated *S. salivarius* HBC12 ($1/\lambda = 0.7$ nm). Unfortunately, both dynamic light scattering and particulate microelectrophoresis provide indirect indications of the cell surface softness. In addition, to visualize fibrillar surface appendages on streptococci by electron microscopy, bacteria have to be negatively stained, and whether or not fibrils are eventually strongly visualized depends on the type of stain employed (Handley, 1990).

After its invention in 1986 (Binnig et al., 1986), it was soon realized that atomic force microscopy (AFM) would be a powerful tool for mapping the surface morphology of biological specimens (Radmacher et al., 1992), including bacterial cell surface layers (Butt et al., 1990; Schabert et al., 1995; Pum and Sleytr, 1996). Besides topographic imaging, AFM makes it possible to probe the local surface forces and mechanical properties of materials (for a review, see Butt et al., 1995). In particular, the mechanical properties of mammalian cells (Weisenhorn et al., 1993; Hoh and Schoenenberger, 1994; Radmacher et al., 1996) and bacterial layers (Xu et al., 1996) have been measured. The large size of microbial cells requires that they be firmly anchored to a substratum for the application of AFM. Kasas and Ikai (1995) proposed a simple and inexpensive solution to

Received for publication 19 July 1999 and in final form 2 February 2000.

Address reprint requests to Dr. H. C. van der Mei, Department of Biomedical Engineering, University of Groningen, Antonius Deusinglaan 1, 9713 AV Groningen, the Netherlands. Tel.: 31-50-3633140; Fax: 31-50-3633159; E-mail: h.c.van.der.mei@med.rug.nl.

0006-3495/00/05/2668/07 $2.00

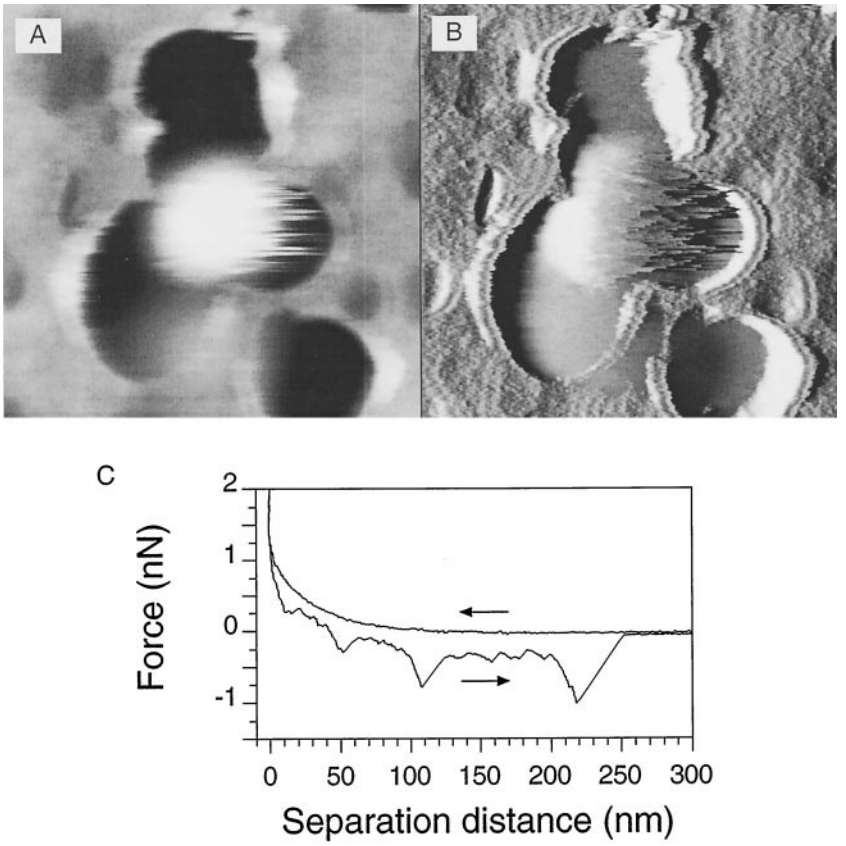

FIGURE 1 AFM gray-scale height (*A*) and deflection (*B*) images (forward scanning; size: 2.5 μm × 2.5 μm; *z* ranges: 500 nm (*A*) and 250 nm (*B*)) and force-distance curve (*C*) recorded for *S. salivarius* HB immersed in water. Note that although the general shape of the retraction force curve did not change dramatically from one measurement to another, variations in the number and location of the adhesion forces were noted. The data are representative of results obtained on at least four cells, using different probes and independent preparations.

achieve this by trapping single cells in a Millipore filter with a pore size comparable with the dimensions of the cell. In this procedure, the highest part of a trapped cell protrudes through the holes of the filter and can easily be probed by AFM. However, hitherto, no validation of AFM results on the softness of cell surfaces by comparison with results from independent techniques has yet been given.

The aim of this paper is to demonstrate the use of AFM to probe the softness of bacterial cell surfaces. To this end, the surfaces of *S. salivarius* HB and HBC12 will be characterized using AFM, including imaging and measurement of force-distance curves, and conclusions drawn will be compared with those derived previously from independent dynamic light scattering and particulate microelectrophoresis.

MATERIALS AND METHODS

Bacterial strains, culture conditions, and harvesting

S. salivarius HB and HBC12 were cultured in Todd Hewitt Broth (Oxoid, Basingstoke, UK) at 37°C in ambient air. For each experiment the strains were inoculated from blood agar in a batch culture. This culture was used to inoculate a second culture that was grown for 16 h before harvesting. Bacteria were harvested by centrifugation (5 min at 5000 × *g*), washed twice with demineralized water, and resuspended in water. To break bacterial chains, cells were sonicated for 30 s at 30 W (Vibra Cell model 375; Sonics and Materials, Danbury, CT). Sonication was carried out intermittently while the cells cooled in an icewater bath. These conditions were found not to damage the cell wall or cause cell lysis.

Atomic force microscopy

Bacterial cells were suspended in water to a concentration of 10^5 per ml, after which 10 ml of this suspension was filtered through an Isopore polycarbonate membrane (Millipore) with a pore size of 0.8 μm (i.e., slightly smaller than the streptococcal dimensions) to immobilize the bacteria through mechanical trapping (Kasas and Ikai, 1995). After filtering, the filter was carefully cut into square sections (1 cm × 1 cm) that were fixed with double-sided sticky tape on a small metal sample disc and transferred into the AFM liquid cell, while avoiding dewetting. AFM imaging and force-distance measurements were made at room temperature, either in deionized water or in 0.1 M KCl solutions, using an optical lever microscope (Nanoscope III; Digital Instruments, Santa Barbara, CA). Contact-mode topographic images were taken with an applied force maintained below 2 nN at a scan rate of ~2 Hz. Oxide-sharpened microfabricated Si_3N_4 cantilevers from Park Scientific Instruments (Mountain View, CA) with a spring constant of 0.03 N m^{-1} and a probe curvature radius of 20 nm (according to manufacturer specifications) were used. Force measurements were made by positioning the tip over individual cells and acquiring a set of force curves. Images were recorded simultaneously in both height and deflection modes, with integral and proportional gains of the feedback loop of 4 and 5, respectively.

At least four cells were measured with the use of different probes and independent preparations, and 10 force-distance curves were recorded for each cell.

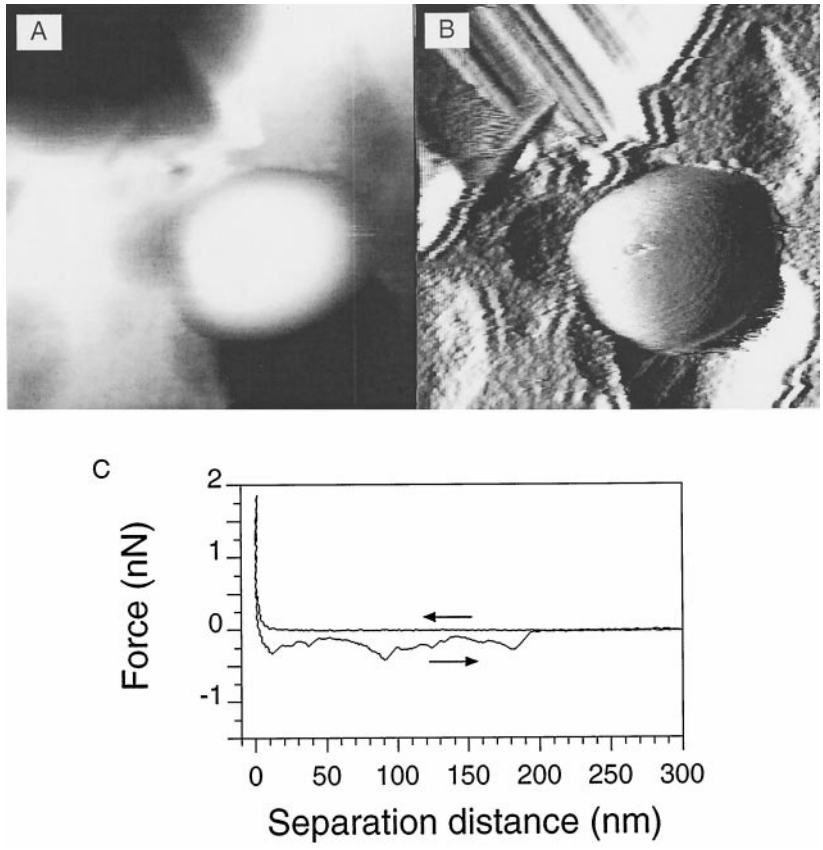

FIGURE 2 AFM gray-scale height (*A*) and deflection (*B*) images (size: 1.5 μm $\times$ 1.5 μm; *z* ranges: 500 nm (*A*) and 100 nm (*B*)) and force-distance curve recorded for *S. salivarius* HB immersed in 0.1 M KCl.

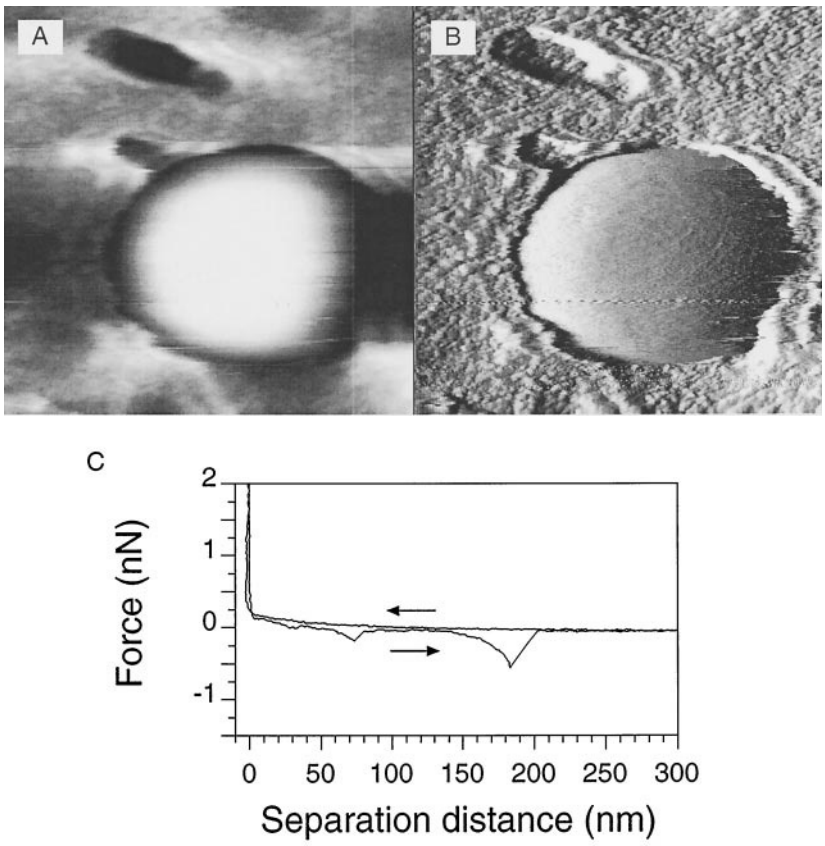

FIGURE 3 AFM gray-scale height (*A*) and deflection (*B*) images (size: 1 μm $\times$ 1 μm; *z* ranges: 200 nm (*A*) and 100 nm (*B*)) and force-distance curve (*C*) recorded for *S. salivarius* HBC12 immersed in water.

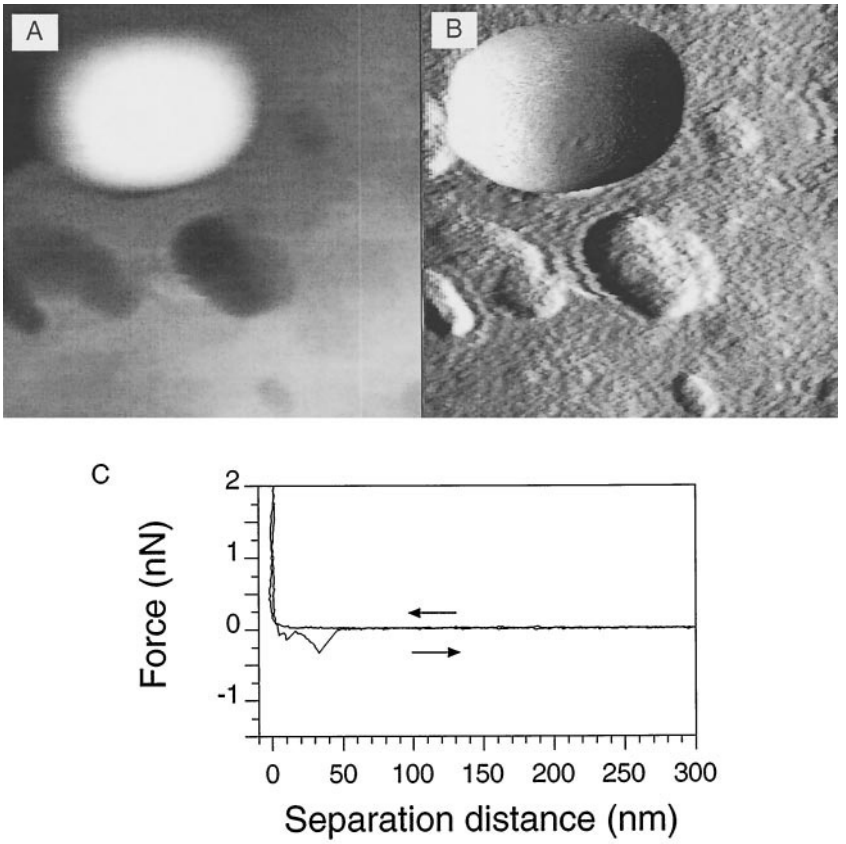

FIGURE 4 AFM gray-scale height (*A*) and deflection (*B*) images (size: 1.5 μm $\times$ 1.5 μm; *z* ranges: 600 nm (*A*) and 150 nm (*B*)) and force-distance curve recorded for *S. salivarius* HBC12 immersed in 0.1 M KCl.

RESULTS

Figs. 1 and 2 present gray-scale height (*A*) and deflection (*B*) images as well as force-distance curves (*C*) obtained for the fibrillated *S. salivarius* HB in water (Fig. 1) and in 0.1 M KCl (Fig. 2). Height images provide quantitative information on sample surface topography, whereas in the deflection images fine surface details can be observed. In water (Fig. 1), images revealed characteristic topographic features on the right-hand side of the cell surface (i.e., lines oriented in the scanning direction). The same area could be imaged repeatedly without apparent alteration of the surface morphology. Images obtained by backward scanning showed similar features, but on the left-hand side of the cell. In contrast, in 0.1 M KCl (Fig. 2) these features could not be detected, indicating a change in the cell surface organization.

These morphological differences were accompanied by differences in the force-distance curves. Upon approach in water (Fig. 1), a long-range repulsion, starting at a separation of ~100 nm, was detected, whereas no jump-to-contact was observed. Upon retraction, multiple adhesion forces were found. The three largest adhesion events were of 0.5–1 nN magnitude and occurred at separation distances of ~50, ~100, and ~220 nm. In 0.1 M KCl (Fig. 2), however, the tip experienced a repulsion upon approach at a much shorter distance, i.e., ~10 nm. Upon retraction in 0.1 M KCl,

TABLE 1 Summary of quantitative data on the softness of fibrillated *S. salivarius* HB and nonfibrillated *S. salivarius* HBC12, including the hydrodynamic radius determined from dynamic light scattering in low- and high-pH solutions, the softness 1/λ from particulate microelectrophoresis, and the characteristics (decay length λ, range, and interaction force at contact F_0) of the repulsive force recorded between the cell surface and the AFM tip

	Hydrodynamic radius* (nm)		Softness 1/λ†	Repulsive force characteristics					
				Decay length λ′ (nm)		Range (nm)		F_0 (nN)	
S. salivarius	pH2	pH7	(nm)	Water	0.1 M	Water	0.1 M	Water	0.1 M
HB	541	747	1.4	34 ± 7	6 ± 2	104 ± 16	12 ± 3	1.1 ± 0.1	0.6 ± 0.1
HBC12	630	565	0.7	12 ± 3	5 ± 3	21 ± 5	10 ± 4	0.4 ± 0.1	0.3 ± 0.1

*Data from van der Mei et al. (1994).
†Data from Bos et al. (1998).

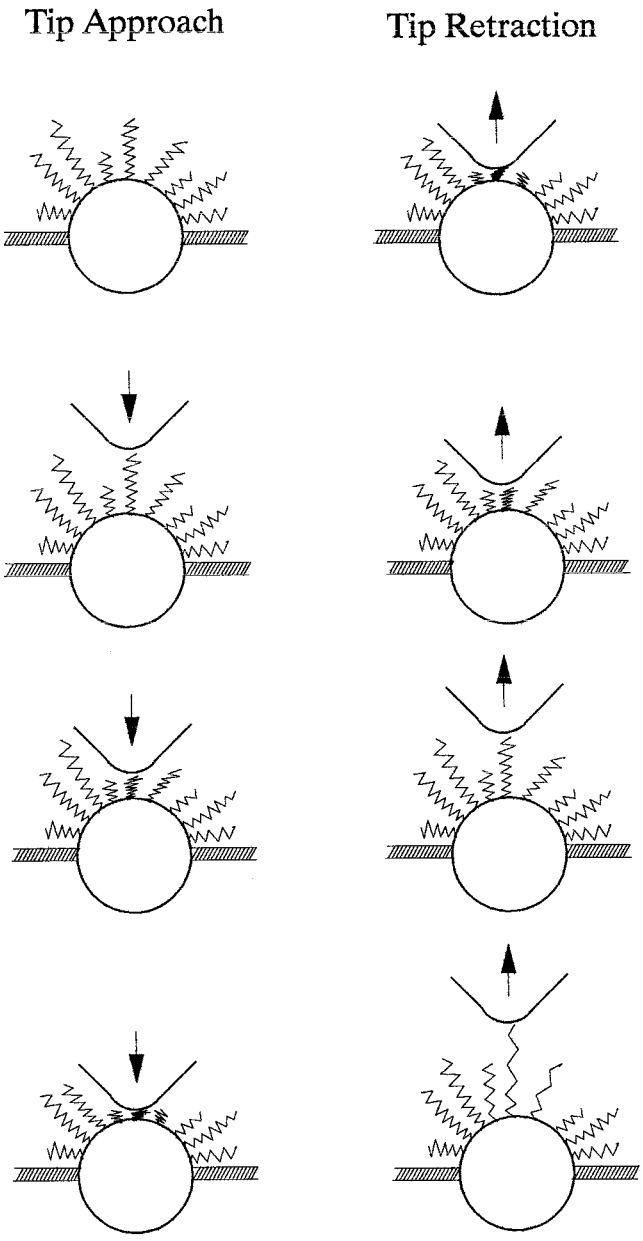

FIGURE 5 Schematic presentation of the potential interaction between an approaching and a retracting AFM tip and different lengths of fibrils on a streptococcal cell surface in water, including stretching of the longest fibril present upon retraction. Adhesion forces are measured each time contact between the tip and a specific length of fibrils is disrupted.

multiple adhesion forces were also observed, but their magnitude was always lower than 0.5 nN.

Gray-scale images and force-distance curves for the nonfibrillated *S. salivarius* HBC12, in water and in 0.1 M KCl, are presented in Figs. 3 and 4, respectively. Images obtained in water did not show the characteristic topographic features seen for the fibrillated strain, while obtained in water and in 0.1 M KCl were nearly identical. Force-distance curves recorded in water and those recorded in 0.1 M KCl were also fairly similar and showed repulsion forces at a separation of 10–20 nm (Figs. 3 and 4). In water, two small (compare Fig. 3 with Fig. 1, for *S. salivarius* HB in water) adhesion forces of 0.1–0.5 nN magnitude were observed, which diminished in magnitude and were located closer to the cell surface in 0.1 M KCl (Fig. 4).

DISCUSSION

Electron microscopy on ruthenium red-stained streptococci has revealed an array of different fibrillar structures with distinct lengths on the cell surface of *S. salivarius* HB. These fibrils had lengths of 72, 91, and 178 nm and were proteinaceous in nature (van der Mei et al., 1987). With electron microscopy, *S. salivarius* HBC12 appeared to have a so-called fuzzy coat around the cell surface consisting of polysaccharides, but no fibrils or other appendages, when stained with ruthenium red. In this paper, the morphology and softness of the proteinaceous, fibrillar cell surface of *S. salivarius* HB are compared, by AFM, with those of the peptidoglycan-rich cell surface of the nonfibrillated *S. salivarius* HBC12. The characteristic topographic features observed on the surface of *S. salivarius* HB in water are associated with the fibrillar structures present on this strain, which is supported by the fact that these features were observed neither on *S. salivarius* HB at high ionic strength, because of collapse of the fibrillar mass, nor on the nonfibrillated *S. salivarius* HBC12 at both low and high ionic strengths.

Differences in surface morphology are directly correlated with differences in interaction forces. The approach curves in Figs. 1–4 can be fitted with an exponential function:

$$F = F_0 e^{-d/\lambda'} \quad (1)$$

in which F is the measured force, F_0 is the force at zero separation distance, d is the separation distance, and λ' is a decay length. Furthermore, a range of the repulsive force may be defined as the distance at which repulsion is first detected. The decay length, the range, and the force at zero separation distance are summarized in Table 1 for both strains suspended in water and in 0.1 M KCl. In addition, Table 1 presents previously obtained data related to the softness of the cell surfaces, as indirectly assessed from dynamic light scattering and particulate microelectrophoresis. The softer cell surface of *S. salivarius* HB is evident here from its greater $1/\lambda$ and the decrease in its hydrodynamic radius with a decrease in pH of the suspending fluid, interpreted as a collapse of the fibrillar mass. *S. salivarius* HBC12, on the other hand, shows a slight increase in its hydrodynamic radius with a decrease in the suspension pH, while $1/\lambda$ is smaller than that of *S. salivarius* HB.

For *S. salivarius* HB at low ionic strength, the long-range repulsion force starting at ~100 nm is attributed to the compression of the soft layer of fibrillar material present at

the cell surface. A close contact between the tip and the cell is achieved only when the applied force exceeds ~1 nN (F_0). The range of the repulsive force at high ionic strength (~10 nm) is much shorter than at low ionic strength, indicating a stiffer surface due to the collapse of the fibrils, in agreement with the topographic images. As can be seen in Table 1, tip-sample contact is established for forces smaller than 1 nN. The shorter repulsion range (10–20 nm) measured for the surface of *S. salivarius* HBC12, at both low and high ionic strength, is indicative of a more rigid surface regardless of ionic strength, which is consistent with the bald cell surface morphology. In this case, the repulsion force may reflect hydration forces associated with the presence of a polysaccharide-rich "fuzzy coat" around the cell surface. After force-distance measurements cells were reimaged to check if cell rupture had occurred, and no differences were found between the images before and after force measurements.

The differences in the cell surface softness of the two streptococcal strains in low- and high-ionic-strength solutions as probed directly by AFM can be interpreted in line with conclusions from dynamic light scattering and particulate microelectrophoresis (see also Table 1). The surface of the nonfibrillated *S. salivarius* HBC12 is "electrophoretically rigid," i.e., $1/\lambda$ is small, and dynamic light scattering did not show a decrease in hydrodynamic radius with a decrease in the pH of the suspending fluid, as opposed to observations for the fibrillated *S. salivarius* HB strain.

Furthermore, it is interesting to note that retraction curves in Fig. 1 for *S. salivarius* HB show multiple adhesion forces at separation distances of 50, 100, and 220 nm. Hypothetically, these adhesion forces might be due to interactions between the AFM tip and different lengths of fibrils on the cell surface, as explained schematically in Fig. 5, although the separation distances at which these adhesion forces occur do not exactly match the lengths of fibrils (72, 91, and 178 nm) determined by electron microscopy. This interpretation would require that interaction between the 178-nm-long fibrils and the AFM tip yields stretching of this fibrillar class, as the most remote adhesion force measured for *S. salivarius* HB occurs at 220 nm.

CONCLUSION

This paper demonstrates the use of AFM to study, in a direct way, the surface softness of microbial cells by comparing fibrillated and nonfibrillated *S. salivarius* strains, previously shown as being soft and more rigid by dynamic light scattering and particulate microelectrophoresis. The fibrillated strain imaged in water shows characteristic topographical features attributable to fibrils. These are not observed for that strain at high ionic strength or for the nonfibrillated strain at both low and high ionic strengths. These morphological differences correlate with major differences in the force-distance curves: 1) the fibrillated strain in water shows a long-range repulsion force upon approach, reflecting compression of the fibril layer; 2) at high ionic strength, the repulsion range is clearly smaller, indicating an increase in sample stiffness due to collapse of the fibrillar mass; 3) the nonfibrillated strain, in both low- and high-ionic-strength solutions, shows a much smaller repulsion range, and thus a much stiffer surface, than the fibrillated strain in water.

The authors thank P. Grange for the use of the atomic force microscope and P. G. Rouxhet for valuable discussions.

The support of the National Foundation for Scientific Research (FNRS), the Foundation for Training in Industrial and Agricultural Research (FRIA), and the Federal Office for Scientific, Technical and Cultural Affairs (Interuniversity Poles of Attraction Programme) is gratefully acknowledged.

REFERENCES

Binnig, G., C. F. Quate, and Ch. Gerber. 1986. Atomic force microscope. *Phys. Rev. Lett.* 56:930–933.

Bos, R., H. C. van der Mei, and H. J. Busscher. 1998. "Soft-particle" analysis of the electrophoretic mobility of a fibrillated and nonfibrillated oral streptococcal strain: *Streptococcus salivarius. Biophys. Chem.* 74:251–255.

Busscher, H. J., P. S. Handley, R. Bos, and H. C. van der Mei. 2000. Physico-chemistry of microbial adhesion from an overall approach to the limits. *In* Physical Chemistry of Biological Interfaces. A. Baszkin and W. Norde, editors. Marcel Dekker, New York. 431–458.

Butt, H.-J., K. H. Downing, and P. K. Hansma. 1990. Imaging the membrane protein bacteriorhodopsin with the atomic force microscope. *Biophys. J.* 58:1473–1480.

Butt, H.-J., M. Jaschke, and W. Ducker. 1995. Measuring surface forces in aqueous electrolyte solution with the atomic force microscope. *Bioelectrochem. Bioenerg.* 38:191–201.

Handley, P. S. 1990. Structure, composition and functions of surface structures on oral bacteria. *Biofouling.* 2:239–264.

Hoh, J. H., and C.-A. Schoenenberger. 1994. Surface morphology and mechanical properties of MDCK monolayers by atomic force microscopy. *J. Cell Sci.* 107:1105–1114.

Kasas, S., and A. Ikai. 1995. A method for anchoring round shaped cells for atomic force microscope imaging. *Biophys. J.* 68:1678–1680.

Ohshima, H. 1994. Electrophoretic mobility of soft particles. *J. Colloid Interface Sci.* 163:474–483.

Ohshima, H. 1995. Electrophoretic mobility of soft particles. *Colloids Surf. A Physicochem. Eng. Aspects.* 103:249–255.

Ohshima, H., and T. Kondo. 1991. On the electrophoretic mobility of biological cells. *Biophys. Chem.* 39:191–198.

Pum, D., and U. B. Sleytr. 1996. Molecular nanotechnology and biomimetics with S-layers. *In* Crystalline Bacterial Cell Surface Proteins. U. B. Sleytr, P. Messner, D. Pum, and M. Sára, editors. R. G. Landes, Austin, TX. 175–209.

Radmacher, M., M. Fritz, C. M. Kacher, J. P. Cleveland, and P. K. Hansma. 1996. Measuring the viscoelastic properties of human platelets with the atomic force microscope. *Biophys. J.* 70:556–567.

Radmacher, M., R. W. Tillmann, M. Fritz, and H. E. Gaub. 1992. From molecules to cells: imaging soft samples with the atomic force microscope. *Science.* 257:1900–1905.

Schabert, F. A., C. Henn, and A. Engel. 1995. Native *Escherichia coli* OmpF porin surfaces probed by atomic force microscopy. *Science.* 268:92–94.

van der Mei, H. C., J. M. Meinders, and H. J. Busscher. 1994. The influence of ionic strength and pH on diffusion of microorganisms with different structural surface features. *Microbiology.* 140:3413–3419.

van der Mei, H. C., A. H. Weerkamp, and H. J. Busscher. 1987. Physicochemical surface characteristics and adhesive properties of *Streptococcus salivarius* strains with defined surface structures. *FEMS Microbiol. Lett.* 40:15–19.

Weisenhorn, A. L., M. Khorsandi, S. Kasas, V. Gotzos, and H.-J. Butt. 1993. Deformation and height anomaly of soft surfaces studied with an AFM. *Nanotechnology.* 4:106–113.

Xu, W., P. J. Mulhern, B. L. Blackford, M. H. Jericho, M. Firtel, and T. J. Beveridge. 1996. Modeling and measuring the elastic properties of an archaeal surface, the sheath of *Methanospirillum hungatei*, and the implication for methane production. *J. Bacteriol.* 178:3106–3112.